Multiplexed PCR to measure *in situ* growth rates of uropathogenic *E. coli* during experimental urinary tract infection.

Santosh Paudel[1], Geoffrey B. Severin[1], Ali Pirani[1], Evan S. Snitkin[1,2], Harry L.T. Mobley[1*]
[1]Department of Microbiology and Immunology, and
[2]Department of Internal Medicine, University of Michigan Medical School, Ann Arbor, USA

*corresponding author

Abstract

Measuring bacterial growth rates *in vitro* is routine, however, determining growth rates during infection in host has been more challenging. Peak-to-trough ratio (PTR) is a technique for studying microbial growth dynamics, calculated using the ratio of replication origin (*ori*) copies to that of the terminus (*ter*), as originally defined by whole genome sequencing (WGS). WGS presents significant challenges in terms of expense and data analysis complexity due to the presence of host DNA in the samples. Here, we used multiplexed PCR with fluorescent probes to estimate bacterial growth rates based on the abundance of *ori*- and *ter*-adjacent loci, without the need for WGS. We establish the utility of this approach by comparing growth rates of the uropathogenic *Escherichia coli* (UPEC) strain HM86 by WGS (PTR) and qPCR to measure the equivalent *ori:ter* ($O:T^{PCR}$). We found that PTR and $O:T^{PCR}$ were highly correlated and that $O:T^{PCR}$ reliably predicted growth rates calculated by conventional methods. $O:T^{PCR}$ was then used to calculate the *in situ E. coli* growth rates in urine, bladder, and kidneys collected over the course of a week from a murine model of urinary tract infection (UTI). These analyses revealed that growth rate of UPEC strains gradually increased during the early stages of infection (0–6h), followed by a slow decrease in growth rates during later time points (1-7 days). This rapid and convenient method provides valuable insights into bacterial growth dynamics during infection and can be applied to other bacterial species in both animal models and clinical infections.

Importance

Accurately measuring bacterial growth rates in the host, which plays a crucial role in determining the success of pathogens in establishing infections, poses significant challenges. To address this, bacterial replication rate has been measured as a proxy for growth rate estimation. While whole genome sequencing (WGS) has been used for this purpose, it comes with drawbacks such as high costs and difficulties in analyzing bacterial sequences due to the overwhelming presence of host DNA. In this study, we validate a more accessible PCR-based approach compared to the established WGS method and confirmed the reliability of our PCR-based technique. We then applied it to measure the growth rate of *Escherichia coli* during an experimental urinary tract infection in a mouse model. This study provides a cost-effective and efficient alternative

41 to WGS for studying bacterial replication dynamics during infection, potentially offering
42 new insights into pathogen behavior and host-microbe interactions.

Introduction

Urinary tract infections (UTIs) are among the most prevalent bacterial infections, with *Escherichia coli* being the primary causative agent constituting approximately 75% of uncomplicated UTIs and 65% of complicated UTI cases (1). While the virulence factors and pathogenicity of uropathogenic *E. coli* (UPEC) (1–3), the *in vivo* growth dynamics during UTIs remain less understood. Bacterial replication rate is important to pathogenicity as it can influence evasion of the host response, colonization, and persistence (4). Understanding bacterial growth rates at different infection niches will also advance our knowledge of how each unique environment affects bacterial proliferation and the progression of infection and help pinpoint specific factors responsible for promoting or inhibiting bacterial growth.

Recent studies have established the use of bacterial circular chromosome replication as a means to determine growth rates with the underlying principle that rapidly growing bacteria have multiple replication forks starting at the origin (*ori*), leading to greater abundance of DNA proximal to the *ori* than distal sequences located near the terminus (*ter*) whereas slow growing or stationary phase bacteria have a more equitable number of *ori* and *ter* loci (Fig. 1). The ratio of sequencing coverage between the *ori* and *ter*, obtained from whole genome sequencing (WGS), is referred to as the peak-to-trough ratio (PTR) and was first applied by Korem *et al*. in 2015 for the determination of bacterial growth rates in a metagenomic study (5). Subsequently, a number of studies have utilized the concept of PTR to measure bacterial growth rates in a variety of conditions using WGS (5–12), digital droplet PCR (13), and SYBR green dye-based quantitative real time PCR (qPCR) (14). While WGS-based PTR has been widely applied and allows for the quantification of both *ori* and *ter* adjacent sequence abundance within the same sample, this method is expensive, requires computational resources and expertise, and generates an unnecessary amount of sequencing data if growth rate determinations are the sole objective. While techniques utilizing qPCR-based methods offer a more economical approach to specifically quantify *ori* and *ter* adjacent sequences, their reliance non-specific DNA-intercalating dyes necessitates the quantification of *ori* and *ter* abundance in the same sample be measured independently from one another. In our study, we combine both the ease of in-house qPCR with the WGS benefit of simultaneous measurement of *ori* and *ter* abundance in the same sample reaction by multiplexing qPCR reactions using TaqMan probes, we call $O{:}T^{PCR}$.

The purpose of this study was two-fold: 1) To develop a probe-based multiplexed qPCR method for measuring *ori:ter* and 2) to use this method to determine the growth rates of UPEC strains *in vivo* during experimental urinary tract infection in mice. Validation of this approach streamlines the process of determining *ori:ter* to accurately and rapidly estimates doubling times in diverse biological samples. Measuring bacterial growth rate *in vivo* within host tissue may provide insight into the dynamics of experimental infections over time and the possibly clinical outcomes. After validating our qPCR method with conventional PTR measured by WGS, we determined the growth dynamics

of two UPEC strains HM56, and HM86 *in vivo* during experimental murine UTI for 7 days post infection. We found both UPEC strains rapidly replicating in murine urine sample early in the infection (6–12 hpi) with grow rates slowly decreasing through the course of a week. This study demonstrates the usefulness of applying a probe-based qPCR method to measure UPEC growth rates in a clinically relevant model of UTI, which could be leveraged for use in various types of infections and models.

Materials and methods

Bacterial strains and culture conditions

E. coli strains HM56 and HM86 were isolated from cases of uncomplicated UTI and have been described elsewhere (15, 16). Bacterial strains were revived from the frozen stock (-80°C) by culturing overnight in Lysogeny broth (LB), aerating at 200 rpm at 37°C. To conduct an *in vitro* experiment, the HM86 strain was cultured overnight with aeration at 37°C in LB, and inoculated 1:100 in fresh LB, terrific broth (TB), and M9 minimal growth medium supplemented with 0.4% glucose ($M9_{Glc}$). We sampled bacteria from the culture at 0, 1, 1.5, 2, 2.5, 3, 3.5, 4, 5, and 6h to assess bacterial growth rate in different growth media, measuring absorbance (OD_{600}) in cuvettes using GENESYS 10S VIS spectrophotometer (Thermo Scientific). We collected bacterial pellets for each time point by centrifugation at 17K x *g* (Fisher Accuspin Micro 17R) for genomic DNA. The bacterial pellet was immediately placed in dry ice and stored at -80°C until further processing. Bacterial growth rate was determined using the formula:

Growth rate (GR_p) = $(\log(OD_{p+t}/OD_{p-t}))/dt$, where “p” is the time point whose $O{:}T^{PCR}$ values is correlated with the growth rate, “p-t” is the initial OD, “p+t” is the final OD, “dt” is the time elapsed between initial and final OD. For our growth rate calculation, t=30 minutes. Bacterial doubling time (DT) *in vitro* was calculated as $[\log(2)/GR_p]$.

Quantitative polymerase chain reaction (qPCR)

Genomic DNA (DNA) from *in vitro* bacterial culture samples and mice urine and organs were extracted using DNeasy® Blood and Tissue Kit (Qiagen, Germany) following manufacturer’s instruction. The qPCR was performed to determine the *ori:ter* ratio, a proxy of PTR (referred in this study as $O{:}T^{PCR}$). The DNA concentration was estimated using Nanodrop One (Thermo scientific). The bacterial DNA in concentration of 500 pg was used to determine PTR for the *in vitro* samples. The targeted nucleotide sequences for the qPCR reaction near the origin of the replication (*ori*) is the *gidA* gene, and near the terminus of replication (*ter*) is the *dcp* gene.

The qPCR reaction was performed in QuantStudio 3 (Applied Biosystems) thermocycler (95°C 30 s, 40×(95 °C 5 s+58 °C 30 s). The optimized 25 µl reaction mixture contained 12.5 µl TaqMan™ Fast Advanced Master Mix (Applied biosystems), 2.5 µl template DNA, and 10 µl of the reaction mixture of forward and reverse primer for *ori* and *ter* region (final primer concentration 1µM each), and probe for *ori* and *ter* sequence (concentration 0.25µM each). To ensure the reliability and accuracy of the qPCR results,

123 we repeated certain samples using a second set of primers that targeted the same
124 region with the same probes for both set of primers. Primers (14, 17) and probes used
125 for qPCR are provided in Table 1. The $O:T^{PCR}$ was determined using $2^{-\Delta\Delta Ct}$ method
126 ($\Delta Ct = Ct_{ori} - Ct_{ter}$; $\Delta\Delta Ct = \Delta Ct_{test} - \Delta Ct_{reference}$). The PTR for each sample is the average
127 PTR of 3 technical replicates. The sample of the same bacterial strain cultured to
128 stationary phase of growth, whose peak-to-trough is expected to be 1, is used for the
129 normalization during each run. To evaluate the specificity of the primers and probes
130 utilized in the experiment we performed two experiments: 1) using DNA from various
131 Gram-positive and Gram-negative bacteria, both individually and mixed with *E. coli* DNA
132 (1:1) to determine whether the presence of DNA from other bacterial sources affect the
133 *ori:ter* ratio, and 2) inclusion of DNA extracted from murine kidney to assess the *E. coli*
134 DNA-specificity of the qPCR in the presence of mouse genetic material. Molecular
135 biology grade water (Corning) was used as non-template control (NTC) for each cycling
136 run. The sample tested for PTR using WGS was incorporated in every set of the qPCR
137 performed to minimize the experimental variability in PTR measurements between
138 experiments. The qPCR assay was performed for the UPEC strains cultured *in vitro* in
139 LB, TB, $M9_{Glc}$ and *in vivo* samples from the mouse during UTI.

140 **Whole genome sequencing**

141 PTR values were determined using previously published methods (5, 6). Briefly,
142 sequenced reads from each sample were cleaned and mapped to the complete genome
143 sequence of the originating bacterial isolate using Trimmomatic v0.39 and Bowtie2
144 v2.5.1. All alignments were indexed and sorted using SAMtools v1.18, and the coverage
145 depth for each nucleotide position was extracted using Bedtools v2.30.0. A smoothing
146 filter was applied to the mapped coverage of genomic segments, which was comprised
147 of a moving sum with a window size of 10 kbp and a slide of 100 bp, followed by a
148 moving median with a window size of 10-kbp bins and a slide of 100 bins. Instances
149 where the bins did not have any mapped reads or had <50% remaining bins were
150 discarded. The PTR was calculated from the peak and trough read coverage locations
151 corresponding to maximum and minimum values, respectively, from the smoothed
152 coverage (5). Snakemake implementation and analysis results can be accessed
153 at https://github.com/alipirani88/Growth-rate-estimate_SMAKE. Assemblies for HM86
154 and HM68 were generated with Flye 2.9.2 and annotated with Prokka 1.14.5. Origin and
155 termination of replication sites were determined by blasting qPCR OriC and Ter loci
156 using BLAST 2.14.0

157 **Mouse model of ascending UTI**

158 Six-to-eight weeks old female CBAJ (Jackson laboratory) mice were inoculated
159 transurethrally with ~$2x10^8$ CFUs of UPEC strains as described previously (18, 19).
160 Briefly, the overnight culture of UPEC strains cultured with shaking at 37°C was
161 centrifuged for 30 minutes at 3000 rpm and the bacterial pellet was resuspended in
162 sterile PBS. Mice were anaesthetized using ketamine/xylazine intraperitoneally (IP).

Then, 50 µl of bacterial suspension was inoculated transurethrally using a sterile polyethene catheter connected to an infusion pump (Harvard Apparatus). After the induction of the UTI, urine samples from the inoculated mice were collected at 6, 24, 48, 72, 96, 120, 144, and 168 hpi for determination of CFUs and isolation of bacterial DNA. Mice were euthanized at 6, 24, and 168 hpi, and bladder and kidneys were collected for bacterial burden and bacterial DNA in the tissue samples. The bladder, and kidneys were collected in 5 ml culture tubes with 2 ml of ice-cold sterile PBS and homogenized using homogenizer (GLH 850, OMNI International). Bacterial burden from urine and each organ were enumerated using dilution plating by the drip-plate method and incubation at 37˚C. The limit of detection (LOD) of bacteria in urine was 10^3 CFU/ml, whereas for bladder and kidney is 20 CFU/organ. Urine and tissue homogenates were centrifuged at 17K x *g* at 4°C for 5 minutes. The supernatant was discarded, and the pellet was placed immediately on dry ice and stored at -80°C until further processing for DNA to measure bacterial growth rate determining PTR.

Statistical analysis

Correlations between PTR and $O{:}T^{PCR}$, and bacterial growth rate and $O{:}T^{PCR}$ were evaluated using Pearson's correlation coefficient. Linear regression analysis was performed to establish the relationship between growth rate and $O{:}T^{PCR}$. Statistical significance of the doubling time (DT) measured by OD and PTR was determined using the paired *t*-test. Statistics and illustrations were performed using GraphPad Prism version 10 (GraphPad Software, CA, USA). A two-tailed *p*-value < .05 was considered statistically significant.

Results

Validating multiplexed quantitative real time PCR with whole genome sequencing as a tool for measuring origin to terminus ratios *in vitro*

To compare WGS PTR with our qPCR *ori:ter* method, we first generated a standard curve relating the growth rates of bacterial populations cultured *in vitro* to the relative abundance of the corresponding *ori* and *ter* sequences. This was achieved by culturing the *E. coli* strain HM86 in three different media where rapid and slow bacterial growth could be observed: lysogeny broth (LB), terrific broth (TB) and an M9 minimal medium containing glucose ($M9_{Glc}$). Growth curves were initiated by addition of a one-to-one-hundred dilution of stationary phase HM86 culture into fresh medium and the optical density (OD_{600}) of the bacterial population was measured at 30 to 60 minutes intervals over the six-hour period. Concurrent with these OD_{600} measurements, cell pellets were collected for genomic DNA extraction from which the relative abundance of the *ori* and *ter* sequences in the bulk population were measured by both multiplexed qPCR and WGS.

As anticipated, *E. coli* HM86 grew rapidly in both rich media conditions (LB and TB) (Fig. 2 A) achieving exponential growth as early as 1.5 h post-inoculation and transitioning into stationary phase approximately two-hours later. In contrast, growth in

203 $M9_{Glc}$ was markedly slower with a longer lag phase and achieving a greatly reduced
204 bacterial density over the course of six hours (Fig. 2A).

205 We first performed WGS on DNA samples collected throughout these growth curves to
206 measure the relative abundance of *ori* and *ter* regions. Figure 2B illustrates one such
207 read coverage plot from *E. coli* HM86 cultured in LB medium (Fig. 2A). During periods
208 of rapid population expansion (1 – 3 h), we observed higher sequencing coverage (*i.e.*,
209 peak) around the *ori* and lower sequencing coverage (*i.e.*, trough) corresponding with
210 the location of the *ter*. As expansion of the population slowed, the relative abundance of
211 reads mapping to the *ori* and *ter* regions normalized, resulting in a PTR of ~1. Plotting
212 the PTR from WGS data across the rich media growth conditions (Fig. 2C) illustrates
213 the dynamic transition in PTR throughout the course of the growth curves (LB and TB, n
214 = 3) with mean maximal PTR being observed at 1.5 h (LB = 1.68 ± 0.14, TB = 1.73 ±
215 0.1). While WGS was only performed for a single population of *E. coli* HM86 cultured in
216 low nutrient $M9_{Glc}$, the very modest changes in PTR predictably corresponded to the
217 slow increase in culture density over time with a maximal PTR of 1.28 at 6 h (Fig. 2A).

218 We next tested whether multiplexing qPCR was a viable alternative to WGS for
219 measuring the relative abundance of *ori* and *ter* sequences using these same *in vitro*
220 DNA samples. Using previously published primers (14) and newly designed probes
221 specific for regions near the *ori* and *ter,* we were able to rapidly generate *ori:ter* ($O:T^{PCR}$
222) for *E. coli* HM86 cultured in all three media (Fig. 2D). Similar to PTR (Fig. 2B), the
223 relative *ori:ter* measured by $O:T^{PCR}$ in rich media were greatest during times of rapid
224 population expansion with mean maximal *ori:ter* measured at 1.5 h (LB = 2.56 ± 0.12,
225 TB = 2.69 ± 0.28) and this ratio gradually normalized to ~1 as cultures reached
226 stationary phase (Fig. 2A). We also observed that the *ori:ter* in $M9_{Glc}$ also demonstrated
227 a modest change in the $O:T^{PCR}$ reflective of the slow and limited expansion of the *in vitro*
228 population over time (Fig. 2A) with a mean maximal *ori:ter* of 1.43 ± 0.05 measured at
229 3.5 h. While the relationship between the *ori:ter* and *in vitro* culture growth phases were
230 similar between PTR and $O:T^{PCR}$ in all three media, the maximal values of the *ori:ter*
231 during times of population expansion were greater when measured by multiplexed
232 qPCR than WGS (Figs. 2C & 2D). Despite differences in the absolute values of $O:T^{PCR}$
233 and PTR, we found the measurements *ori:ter* and PTR of each individual DNA sample
234 were highly correlated in all three media conditions (Figs. 2E, 2F & 2G). The difference
235 in absolute magnitude of *ori:ter* is likely reflective of a greater dynamic range in
236 measuring *ori* and *ter* abundance by multiplexed qPCR and correlation of these
237 measurements with PTR demonstrates the viability of using probe-based qPCR in lieu
238 of WGS.

239 **$O:T^{PCR}$ accurately predicts bacterial growth rate *in vitro***

240 Having demonstrated $O:T^{PCR}$ is a reliable method to measure *ori:ter*, we then calculated
241 growth rates for each time point across every growth curve based on the OD_{600}
242 measurements that immediately preceded and followed that time point. A standard
243 curve of growth rate and $O:T^{PCR}$ was then established from all time points where the

244 median growth rate from biological replicates cultured in same medium was less than
245 0.0025 (*i.e.*, doubling time of 120 min) (Fig. 3A). This minimum doubling time criterion
246 functionally incorporated all regions of the three growth curves where active growth
247 could be observed (*i.e.*, excluded lag and stationary phases) and the O:T^{PCR} were in
248 excess of 1.25 and these time points are illustrated as filled symbols in Fig. 1A and 1D.
249 From these data, we could construct a standard curve and derive a linear equation
250 (Y=0.007648*X-0.006786) based on the relationship between growth rate and O:T^{PCR}
251 (Fig. 3A). We then used this equation to calculate a predicted growth rate for all O:T^{PCR}
252 measurements included in the standard curve and found no significant difference
253 between the predicted growth rate and the experimentally derived growth from OD_{600}
254 measurements for each O:T^{PCR} measurement (Fig. 3B). The constraints of this standard
255 curve are the maximum and minimum O:T^{PCR} measurements of 2.87 and 1.16
256 representing a doubling times of 19.9 and 143.0 minutes, respectively. Therefore,
257 O:T^{PCR} which are greater or less than these extremes cannot be used to accurately
258 determine bacterial growth rates and are instead defined as extremely rapid growth or
259 slow growth, respectively.

260 **Establishing limits of *ori:ter* quantification, detection, and specificity of O:T^{PCR}**

261 Under optimal conditions, such as bacterial monoculture, bacterial DNA can be
262 extracted, quantified, and used in downstream molecular applications with the
263 knowledge that all the nucleic acids present originated from a single source. In an
264 infection model, DNA extracted from a complex biological sample will be a mixture of
265 both host and etiological agent derived nucleic acids. Additionally, the concentration of
266 bacterial DNA within this sample will be unknown and likely to be in low abundance.
267 Therefore, we established two constraints for accurate *ori:ter* determination by O:T^{PCR} in
268 complex biological samples: a limit of quantification (LOQ) establishing the minimum
269 number of CFU (LOQ-CFU) from which DNA could be extracted and accurately
270 measured, and LOQ-DNA demonstrating the minimum quantity of bacterial DNA which
271 can be accurately measured.

272 Because the total number of CFU collected in a biological sample from an infection model
273 can vary, we chose to establish LOQ which would represent the minimum number of
274 bacterial cells required to provide adequate template DNA for accurate O:T^{PCR}
275 determination. To establish this LOQ, we cultured *E. coli* HM86 to exponential phase in
276 LB for 2 h from which 10-fold serial dilutions were prepared and DNA extractions of ~10^6,
277 10^5, 10^4, 10^3, 10^2, 10, and 0 CFUs were performed. From these DNA extractions we found
278 the relationship between *ori* and *ter* was measured to be approximately 2.23±0.09 by
279 O:T^{PCR} from templates originating from extractions containing 10^6 to 10^3 CFU, while those
280 extracted from fewer CFU resulted in a significant deviation in this ratio (Fig. 4A).
281 Therefore, an LOQ of ≥ 10^3 CFU is required to provide sufficient bacterial DNA template
282 for accurate determination of *ori:ter* by O:T^{PCR} .

283 In a biological sample collected from the infection model, bulk DNA extraction is likely to
284 capture DNA from both the infectious agent and the host. This complex mixture of nucleic

acids is likely to obscure the direct quantification of input template prior to its application in O:T^{PCR}. Because template abundance is correlated with critical threshold (Ct) values obtained by qPCR, we sought to define an LOQ based on the greatest Ct value for the *ori* specific oligo primers from which the relationship of *ori:ter* can be reliably determined by O:T^{PCR}. Using DNA extracted from ~10^8 CFUs, described in LOQ experiment above, we performed O:T^{PCR} with 10-fold serial dilutions of template DNA (5 ng to 0.05 pg) to determine the range from which the *ori:ter* could be reliably measured. O:T^{PCR} containing 5 ng to 0.5 pg template DNA consistently measured an *ori:ter* of approximately 2.32±0.06, and this ratio deviated as the template abundance fell below this range (Fig. 4B). Over the entire range of templates tested, the *ori* oligo Ct values reliably increased by a mean Ct of 3.41 per 10-fold dilution of template (ideal change is 3.32 Ct per 10-fold dilution). Based on the these observations, we found the highest Ct value (*i.e.*, lowest template abundance) from which *ori:ter* could be determined by O:T^{PCR} was 30.52±0.97 cycles. This LOQ establishes a critical threshold for informing the appropriate conditions for the application of *ori:ter* measured by O:T^{PCR}; where the *ori* oligo Ct≤30.52, the corresponding *ori:ter* can be confidently used to accurately calculate the growth rate of the bacteria in that sample.

As described above, biological samples collected from an infection model are likely to contain at least two sources of DNA; the infectious agent and the host. There also exists the possibility that samples can contain DNA extracted from other sources (*e.g.*, host commensals). To test the specificity of the *ori* and *ter* oligos to discriminate between *E. coli* and from other sources of DNA we performed O:T^{PCR} on mixed DNA templates containing 5 ng of *E. coli* HM86 DNA combined with of 5 ng of DNA isolated from alternative sources. In the absence of extraneous DNA, the template composed of exclusively *E. coli* HM86 DNA had a 16.04±0.13 *ori* oligo Ct and a 2.40±0.03 O:T^{PCR}. Addition of equal amount of DNA template purified from seven Gram-negative species cultured overnight (*Acinetobacter baumannii*, *Citrobacter freundii*, *Enterobacter hormaechei*, *Klebsiella pneumoniae*, *Morganella morganii*, *Pseudomonas aeruginosa*, *Serratia marcescens*), two Gram-positive species (*Bacillus subtilis* and *Staphylococcus aureus*) (Table 2), or host murine DNA (CBAJ) (Fig. 4B) did not significantly affect the detection of the *E. coli* HM86 template. While some reactivity with the *ori* and *ter* oligos was observed in the absence of *E. coli* HM86 DNA template for some of these alternative DNA samples, as well as the matrix control from the purification kit, the observed *ori* oligo Ct values were greater than the established LOQ above (≤30.5 Ct) and would therefore be excluded from further analysis.

From these standardization and specificity experiments (Fig. 4), we found that *ori* and *ter* oligos are specific for *E. coli* HM86, extraction of >10^3 bacterial CFUs is needed to provide enough template for O:T^{PCR}, and a Ct≤30.5 for the *ori* oligos is required to accurately quantify the *ori:ter* in a given sample. By applying these criteria as quality control measures for evaluating bacterial growth rates we can apply O:T^{PCR} to complex biological samples collected from an infection model.

326 To ensure the reliability of our PCR method in measuring *ori:ter* ratios, we validated the
327 same primer oligos with the other *E. coli* strain, HM56. We cultured strain HM56 in LB
328 medium for 6h and measured $O:T^{PCR}$ and found similar results to HM86, where HM56
329 DNA behaves like HM86 DNA indicating that our qPCR method is robust and applicable
330 across different *E. coli* strains (Fig. S1).

331 **Mouse model of ascending UTI**

332 Following parameterization of $O:T^{PCR}$, we applied this method to measure *in vivo* bacterial
333 growth rates in our model of interest, the experimental murine model of ascending UTI,
334 over a period of seven days. For this, we induced experimental UTI in 6–7 week CBAJ
335 female mice by transurethral catheterization and mono-culture inoculation of UPEC
336 strains HM86 and HM56 isolated from uncomplicated female UTI patients (16, 20). Urine
337 samples from the infected mice were collected at 6, 24, 48, 72, 96, 120, 144, and 168 hpi,
338 whereas bladder and kidney samples were collected at 6, 24, and 168 hpi in a separate
339 group of mice for bacterial burden and for extracting DNA and measuring growth rates
340 from the two UPEC strains (Fig. 5).

341 Urine bacterial burden showed distinct patterns of colonization for each strain. *E. coli*
342 HM56 urine samples exhibited higher initial counts at 6hpi, with high abundance of
343 bacterial culture later up to 7 days period. In contrast, *E. coli* HM86 exhibited lower urine
344 bacterial count at 6hpi, increased by 24hpi, and maintained a constant level of
345 persistence throughout the infection period (Fig. 5B). Bladder colonization was similar
346 for both strains, with higher level of colonization at 6hpi, which decreased by 24hpi, and
347 remained at similar level up to 168hpi (Fig. 5C). The kidney colonization differed
348 between the two strains. High level of kidney colonization was observed for *E. coli*
349 HM56 at 6hpi, which was found to be lowered by approximately 10-fold at 168hpi.
350 Conversely, *E. coli* HM86 exhibited limited kidney colonization early during the infection
351 (6 hpi, 1 of 5 mice) which increased in abundance at later time points (24 hpi 2 of 5
352 mice; 168 hpi 3 of 5 mice) (Fig 5D) indicating a slower time to ascension. These findings
353 highlight strain-specific variations in colonization patterns during the progression of UTI,
354 providing insights into the dynamics of bacterial colonization, dissemination, and
355 persistence in the different sites of the urinary tract.

356 **Growth rate of UPEC strains *in vivo* during UTI**

357 Bacterial growth rates for HM86 and HM56 were next measured using DNA extracted
358 from urine, bladder and kidney homogenates from infected animals. The recovery of
359 bacterial DNA from the kidney sample was challenging due to the presence of host
360 genetic material as evidenced by the observed Ct values compared to the recovered
361 number of *E. coli* CFUs. However, the recovery was less affected in bladder and urine
362 samples as observed Ct values were similar to the experiment performed with
363 comparable known CFUs *in vitro* from pure bacterial culture. The DNA was extracted
364 from urine, bladder, and kidney samples and *ori:ter* was determined. Fig. 6 illustrates
365 the *ori:ter* values determined by qPCR from the urine samples during infection over the

366 period of 168h. We observed comparable patterns of *ori:ter* between the two tested
367 strains over the infection timeline, which shows the variability in the replication rate.
368 From this *ori:ter* -values we can predict that the growth rate of UPEC is higher at 6hpi,
369 which gradually decreases over the infection period whose median *ori:ter* values is
370 around our estimated borderline of the slow and fast growth conditions. No statistically
371 significant difference was observed in *ori:ter* -values over the course of time.

372 The bacterial population doubling time was calculated from the qPCR derived *ori:ter*-
373 values using the equation derived from the linear regression analysis of *E. coli* HM86 *in*
374 *vitro* growth rate with their respective *ori:ter* value (Fig. 4D). The calculated *E. coli* DT in
375 mouse urine is presented in Table 2. This DT results revealed a gradual increase in the
376 growth rate of bacteria during the early stages of infection, peaking at 6h, followed by a
377 slow decrease during later days transitioning to slower state of growth at 168hpi. The
378 fastest median DT for *E. coli* HM56 and HM86 is 47.4 and 54.2 minutes, respectively,
379 observed for both at 6 hpi. The fastest growth of *E. coli* HM56 was observed at 24 hpi
380 with a DT of 28.9 minutes, while for *E. coli* HM86, it was found to be 31.3 minutes at
381 6hpi. In case of individual mice, at 6hpi the fastest growth was determined as 31.6, and
382 31.3 minutes for HM56, and HM86 respectively. During the later time points, the UPEC
383 strains exhibited variable growth rates. This trend suggests that UPEC undergoes rapid
384 multiplication in the urine during early stages of UTI, particularly within the first 6h,
385 followed by a gradual slowdown in growth rate. The similarity in growth rate between the
386 two strains implies a similar growth strategy among different UPEC isolates during
387 infection. Due to the presence of lower number of CFUs in most of the bladder, we were
388 only able to determine *ori:ter* in few bladder samples with Ct value within the range of
389 LOQ. For HM86, the DT in bladder was found to be 33.3 minutes at 6hpi (1/5 mice),
390 which was found slower at 24hpi with DT of 61.2 minutes (1/5 mice). No bladder had
391 sufficient CFUs for *ori:ter* determination at 168hpi for HM86. For HM56, in contrast to
392 HM86, we observed slower growth at 6hpi with DT of 63.1 and 71.2 minutes (2/5 mice),
393 which became even slower at 24 and 168 hpi with DT of 76.8 (1/5 mice) and 81.2 (1/5
394 mice) minutes respectively (Fig.S2-C). In contrast to the bladder, the growth rate in
395 kidney was found to be slower at early stage of infection i.e. 6h followed by faster
396 growth at 24 and 168 hpi for both *E. coli* strains. For HM56, the fastest growth rate was
397 determined with DT of 76.6, 40.2, and 43.7 minutes at 6, 24, and 168 hpi, respectively.
398 Since the kidney colonization with HM86 was limited, we were only able to determine
399 the growth rate of 1 kidney samples at 6 and 168 hpi, with DT of 227.9 and 51.9
400 minutes, respectively (Fig. S2-D). Overall, the results revealed the infection-site specific
401 differences in the *E. coli* growth rate over the course of infection period.

402 Discussion

403 In this study, we developed a PCR-based method as a reliable alternative to WGS for
404 determining bacterial growth rate targeting the specific regions near the origin and
405 terminus of replication. As a proof-of-concept, the qPCR method was conducted on *in*
406 *vitro* samples of *E. coli* HM86 cultured in both slow and rapid growth media and

407 validated the *ori:ter* with results obtained from the WGS method. The validation
408 experiments were performed using the bacterial DNA isolated from the cultures grown
409 under controlled laboratory conditions. This method provides an estimate of the
410 population level PTR from the samples where the bacteria are at different stages in their
411 growth cycle. A series of the control experiments were conducted to validate the growth
412 rate measurements by *ori:ter* using qPCR method for bacterial replication rates in host
413 tissues. We determined that >10^3 bacterial CFUs in pure culture condition gives
414 accurate *ori:ter* measurements with the Ct value of *ori* oligos around 30.5, equivalent to
415 0.5 pg of the DNA used for *ori:ter* measurements. Therefore, we consider Ct values of
416 30.5 or higher to be unreliable for determining *ori:ter*. This results ensures that the
417 *ori:ter* measurements remains accurate even when dealing with low bacterial loads in
418 host tissues during infection studies. Using this validated method, we measured the *E.*
419 *coli ori:ter* during experimental UTI from urine, bladder, and kidney samples from mice.
420 DNA extraction and *ori:ter* measurement in urine and bladder samples with the bacterial
421 count above 10^3 CFUs resulted Ct value within the range of cut-off Ct value providing
422 reliable result. This might vary as the recovery of DNA varies between the extraction
423 protocol. Below this threshold, the consistency of the *ori:ter* was compromised,
424 rendering inconsistencies of the result. In terms of DNA concentration, a total DNA
425 amount of 0.5 pg was sufficient to produce a consistent *ori:ter* value, demonstrating the
426 method's high sensitivity. We were only able to measure *ori:ter* from limited bladder
427 samples since only a few bladder samples had sufficient bacterial counts to enable
428 reliable *ori:ter* measurements within reliable range of Ct values. Although the colonized
429 kidney samples had higher number of CFUs count than that required for accurate *ori:ter*
430 measurement, we were not able to measure *ori:ter* from some kidney samples as the Ct
431 values derived from the qPCR method were higher than the cut-off Ct values. This,
432 however, was not due to the interference of the mouse kidney DNA to reading for
433 bacterial DNA as evidenced by the experiment performed by adding 50 ng of the mouse
434 kidney DNA to 0.5 pg of *E. coli* DNA without deviation in the Ct values and *ori:ter*
435 measurements. This might be due to the inability of our DNA extraction protocol to
436 recover enough bacterial DNA from the mouse kidney tissue homogenate.

437 Experiments using two sets of primers targeting the same region yielded similar results,
438 confirming the reliability of the performed method. Since we employed a probe-based
439 qPCR method, it was highly specific in amplifying the target sequence from the intended
440 bacterial species. This approach allows us to amplify and measure two targeted
441 chromosomal regions from a single sample using their specific probes, thereby reducing
442 discrepancies in readings between wells for the replication origin and terminus regions
443 when determining *ori:ter* measurements. This multiplexing capability is advantageous in
444 reducing both costs and result discrepancies compared to running samples in separate
445 wells for the two target regions.

446 From the *in vivo* growth rate experiment during UTI in mouse, we observed active
447 growth in the urine samples with *ori:ter* >1 in all samples. The fastest growth was
448 observed during the early phase of infection for the tested UPEC strains which gradually

slowed during later days. Previously, the growth rate *in vivo* was determined in mouse UTI as well as human patients determining PTR, a sequencing-based method, which revealed that UPEC strains exhibit rapid growth during human UTIs, often matching or exceeding *in vitro* rates (6). Similar to this study, DT in mouse urine and bladder during experimental UTI at 6hpi was determined to be 34.9, and 36.9 minutes respectively, with much slower growth rate at 24hpi (6).To measure the growth rate *in vivo* during UTI, another study employed qPCR-based method targeting *ori* and *ter* region (21) from the urine sample of the infected human patients with UTI, where active growth with day-to-day and inter-patient variability in growth rate was observed (21). Notably, *E. coli* strains isolated from the urinary tract demonstrate significantly higher growth rates in urine compared to fecal isolates, suggesting adaptation to the urinary environment (6). The slow growth observed during the later stage of infection in the urine and bladder might be due to the multifaceted adaptive response to the challenging host environment such as activation of bacterial stress response mechanism, increased pressure from the host immune system, formation of protective biofilm, or the development of metabolically dormant persister cells. By slowing their growth, *E. coli* can manage nutrients to persist in nutrient-limited conditions, evade host immune responses, and maintain a viable population capable of resisting elimination and potentially causing recurrent infections. This strategy underscores the complex interplay between bacterial pathogens and host defenses in the context of chronic or recurring UTIs (22–28). In contrast to urine and bladder, the *E. coli* growth rate in the kidney was found to be higher during later stages of infection which highlights the niche-specific variations in growth pattern within different areas of the urinary system. The distinct growth dynamics in the kidney suggest that this organ provides a unique environment for *E. coli* proliferation as the infection progresses. From the bacterial burden and growth rate results, we did not observe the direct connection between growth rate and total number of CFUs recovered from urine, bladder, and kidneys.

The strategy of measuring *ori:ter* to study bacterial growth rate has been applied in other infection models, such as mouse peritonitis, revealing heterogeneous growth rates within bacterial populations during infection (14), and blood-stream infections (29) showing organ specific pattern of growth rate in multiple bacterial species. The method has also been tested with slower-growing pathogens like *Xylella fastidiosa*, showing promise for assessing growth status in plant and insect vector environments (30). Importantly, this approach has also been applied to predict antibiotic treatment efficacy (31).

In conclusion, our research establishes the effectiveness of a probe-based qPCR method for measuring *ori:ter* and *in situ* determinations of bacterial growth rate in a cost-effective and efficient manner. This approach of measuring bacterial growth rate by PCR has its potential application in various infection models across different bacterial species.

Acknowledgements

We would like to acknowledge the members of the Mobley lab and Bachman Lab for their insightful feedback throughout this project. This work was supported by the funding NIAID R01AI165582 (H.L.T.M.).

References

1. Flores-Mireles AL, Walker JN, Caparon M, Hultgren SJ. 2015. Urinary tract infections: epidemiology, mechanisms of infection and treatment options. Nat Rev Microbiol 13:269–284.

2. Klein RD, Hultgren SJ. 2020. Urinary tract infections: microbial pathogenesis, host–pathogen interactions and new treatment strategies. Nat Rev Microbiol 18:211–226.

3. Subashchandrabose S, Mobley HLT. 2015. Virulence and Fitness Determinants of Uropathogenic Escherichia coli. Microbiol Spectr 3:10.1128/microbiolspec.uti-0015–2012.

4. Smith H. 1990. Pathogenicity and the Microbe in vivo: The 1989 Fred Griffith Review Lecture. Microbiology 136:377–383.

5. Korem T, Zeevi D, Suez J, Weinberger A, Avnit-Sagi T, Pompan-Lotan M, Matot E, Jona G, Harmelin A, Cohen N, Sirota-Madi A, Thaiss CA, Pevsner-Fischer M, Sorek R, Xavier RJ, Elinav E, Segal E. 2015. Growth dynamics of gut microbiota in health and disease inferred from single metagenomic samples. Science 349:1101–1106.

6. Forsyth VS, Armbruster CE, Smith SN, Pirani A, Springman AC, Walters MS, Nielubowicz GR, Himpsl SD, Snitkin ES, Mobley HLT. 2018. Rapid Growth of Uropathogenic Escherichia coli during Human Urinary Tract Infection. mBio 9:10.1128/mbio.00186-18.

7. Szafrańska AK, Junker V, Steglich M, Nübel U. 2019. Rapid cell division of Staphylococcus aureus during colonization of the human nose. BMC Genom 20:229.

8. Gibson B, Wilson DJ, Feil E, Eyre-Walker A. 2018. The distribution of bacterial doubling times in the wild. Proc R Soc B 285:20180789.

9. Brown CT, Olm MR, Thomas BC, Banfield JF. 2016. Measurement of bacterial replication rates in microbial communities. Nat Biotechnol 34:1256–1263.

10. Long AM, Hou S, Ignacio-Espinoza JC, Fuhrman JA. 2020. Benchmarking microbial growth rate predictions from metagenomes. ISME J 15:183–195.

11. Joseph TA, Chlenski P, Litman A, Korem T, Pe’er I. 2022. Accurate and robust inference of microbial growth dynamics from metagenomic sequencing reveals personalized growth rates. Genome Res 32:558–568.

12. Emiola A, Oh J. 2018. High throughput in situ metagenomic measurement of bacterial replication at ultra-low sequencing coverage. Nat Commun 9:4956.

13. Schneiders S, Hechard T, Edgren T, Avican K, Fällman M, Fahlgren A, Wang H. 2021. Spatiotemporal Variations in Growth Rate and Virulence Plasmid Copy Number during Yersinia pseudotuberculosis Infection. Infect Immun 89:10.1128/iai.00710-20.

14. Haugan MS, Charbon G, Frimodt-Møller N, Løbner-Olesen A. 2018. Chromosome replication as a measure of bacterial growth rate during Escherichia coli infection in the mouse peritonitis model. Sci Rep 8:14961.

15. Subashchandrabose S, Hazen TH, Brumbaugh AR, Himpsl SD, Smith SN, Ernst RD, Rasko DA, Mobley HLT. 2014. Host-specific induction of Escherichia coli fitness genes during human urinary tract infection. Proc Natl Acad Sci 111:18327–18332.

16. Sintsova A, Frick-Cheng AE, Smith S, Pirani A, Subashchandrabose S, Snitkin ES, Mobley H. 2019. Genetically diverse uropathogenic Escherichia coli adopt a common transcriptional program in patients with UTIs. eLife 8:e49748.

17. Riber L, Olsson JA, Jensen RB, Skovgaard O, Dasgupta S, Marinus MG, Løbner-Olesen A. 2006. Hda-mediated inactivation of the DnaA protein and dnaA gene autoregulation act in concert to ensure homeostatic maintenance of the Escherichia coli chromosome. Genes Dev 20:2121–2134.

18. Hagberg L, Hull R, Hull S, Falkow S, Freter R, Edén CS. 1983. Contribution of Adhesion to Bacterial Persistence in the Mouse Urinary Tract. Infect Immun 40:265–272.

19. Hagberg L, Engberg I, Freter R, Lam J, Olling S, Edén CS. 1983. Ascending, unobstructed urinary tract infection in mice caused by pyelonephritogenic Escherichia coli of human origin. Infect Immun 40:273–283.

20. Shea AE, Frick-Cheng AE, Smith SN, Mobley HLT. 2022. Phenotypic Assessment of Clinical Escherichia coli Isolates as an Indicator for Uropathogenic Potential. mSystems 7:e00827-22.

21. Haugan MS, Hertz FB, Charbon G, Sahin B, Løbner-Olesen A, Frimodt-Møller N. 2019. Growth Rate of Escherichia coli During Human Urinary Tract Infection: Implications for Antibiotic Effect. Antibiotics 8:92.

22. Chromek M, Slamová Z, Bergman P, Kovács L, Podracká L, Ehrén I, Hökfelt T, Gudmundsson GH, Gallo RL, Agerberth B, Brauner A. 2006. The antimicrobial peptide cathelicidin protects the urinary tract against invasive bacterial infection. Nat Med 12:636–641.

23. Nielsen KL, Dynesen P, Larsen P, Jakobsen L, Andersen PS, Frimodt-Møller N. 2014. Role of Urinary Cathelicidin LL-37 and Human β-Defensin 1 in Uncomplicated Escherichia coli Urinary Tract Infections. Infect Immun 82:1572–1578.

24. Hayes BW, Abraham SN. 2016. Innate Immune Responses to Bladder Infection. Microbiol Spectr 4:10.1128/microbiolspec.uti-0024–2016.

25. Haraoka M, Hang L, Frendéus B, Godaly G, Burdick M, Strieter R, Svanborg C. 1999. Neutrophil Recruitment and Resistance to Urinary Tract Infection. J Infect Dis 180:1220–1229.

26. Haschka D, Hoffmann A, Weiss G. 2021. Iron in immune cell function and host defense. Semin Cell Dev Biol 115:27–36.

27. Ganz T, Nemeth E. 2015. Iron homeostasis in host defence and inflammation. Nat Rev Immunol 15:500–510.

28. Nairz M, Haschka D, Demetz E, Weiss G. 2014. Iron at the interface of immunity and infection. Front Pharmacol 5:152.

29. Anderson MT, Brown AN, Pirani A, Smith SN, Photenhauer AL, Sun Y, Snitkin ES, Bachman MA, Mobley HLT. 2021. Replication Dynamics for Six Gram-Negative Bacterial Species during Bloodstream Infection. mBio 12:10.1128/mbio.01114-21.

30. Sicard A, Castillo AI, Voeltz M, Chen H, Zeilinger AR, Fuente LDL, Almeida RPP. 2020. Inference of Bacterial Pathogen Instantaneous Population Growth Dynamics. Mol Plant-Microbe Interact 33:402–411.

31. Haugan MS, Løbner-Olesen A, Frimodt-Møller N. 2018. Comparative Activity of Ceftriaxone, Ciprofloxacin, and Gentamicin as a Function of Bacterial Growth Rate Probed by Escherichia coli Chromosome Replication in the Mouse Peritonitis Model. Antimicrob Agents Chemother 63:10.1128/aac.02133-18.

586 # List of Tables

587 **Table 1. Primers and probes used in this study**

ID	Target sequence	Sequence	Reference
oriC F1	*gidA*	CGC AAC AGC ATG GCG ATA AC	PMID: 30297723
oriC R1	*gidA*	TTC GAT CAC CCC TGC GTA CA	PMID: 30297723
ter F1	*dcp*	TCA ACG TGC GAG CGA TGA AT	PMID: 30297723
ter R1	*dcp*	TTG AGC TGC GCT TCA TCG AG	PMID: 30297723
UPEC *oriC* Probe	*gidA*	/56-FAM/ACC CAT GAT /ZEN/GTG ATC CGC AGT AAC CTC GAT CGT A/3IABkFQ/	This study
UPEC *ter*C Probe	*dcp*	/5SUN/CGC GCT AAA /ZEN/CCC GCC CTG CTG CTT AT/3IABkFQ/	This study
oriC F2	*gidA*	TCT CGT TTA TGG GCA ATG CG	This study
oriC R2	*gidA*	TGA TTT CTG TCG GCA AAG CG	This study
ter F2	*dcp*	GCG AGC GAT GAA TTA GCC TC	This study
ter R2	*dcp*	GCC TTC ATT CAA CAC CGT GT	This study

588

589

590 **Table 2. Specificity of *ori* and *ter* primers**

Template DNA source	$O:T^{PCR}$ (mean±SD)	Ct_{ori} (mean±SD)	Ct_{ter} (mean±SD)
E. coli	2.40±0.03	16.04±0.13	17.01±0.11
E. coli + Citrobacter freundii	2.44±0.07	16.08±0.12	17.07±0.08
E. coli + Klebsiella pneumoniae	2.61±0.16	15.94±0.09	17.03±0.04
E. coli + Serratia marcescens	2.57±0.04	16.00±0.03	17.08±0.01
E. coli + Proteus mirabilis	2.35±0.05	16.18±0.01	17.12±0.05
E. coli + Acinetobacter baumanii	2.57±0.02	15.89±0.16	16.96±0.14
E. coli + Enterobacter hormaechei	2.47±0.09	16.08±0.03	17.09±0.07
E. coli + Morganella morganii	2.46±0.03	16.01±0.07	17.02±0.06
E. coli + Pseudomonas aeruginosa	2.43±0.07	16.09±0.04	17.08±0.08
E. coli + Bacillus subtilis	2.41±0.03	16.09±0.12	17.07±0.14
E. coli + Staphylococcus aureus	2.46±0.19	15.93±0.18	16.93±0.08

591

592

593

594

595

Table 3. *E. coli* doubling time in murine urine during experimental UTI

	Doubling time (minutes) [Median (Min-Max)]	
Hours post-infection (hpi)	HM56	HM86
6	47.4 (31.6-105.2)	54.2 (31.3-90.5)
24	64.2 (28.9-153.1)	67.6 (38.3-142.5)
48	65.5 (36.8-70.9)	70.4 (46.9-89.1)
72	68.9 (59.8-148.0)	63.6 (42.0-99.7)
96	68.6 (55.3-128.1)	73.1 (64.5-76.8)
120	60.1 (46.4-70.1)	56.3 (40.8-80.5)
144	65.8 (58.5-68.4)	86.1 (52.8-104.1)
168	90.9 (63-129.1)	75.8 (46.5-139.2)

610 Figures

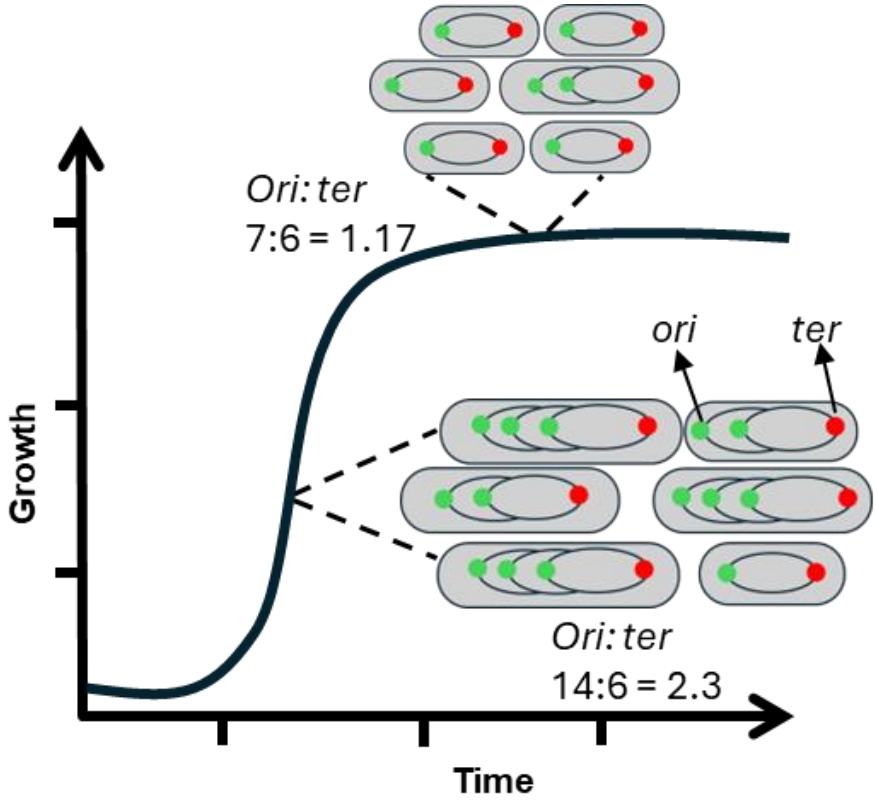

611

612

Fig. 1. Determination of growth rate by PTR. Stages of bacterial growth representing their ori: ter (one of the examples of *ori: ter* during exponential and stationary phase is shown. *ori, green; ter, red*).

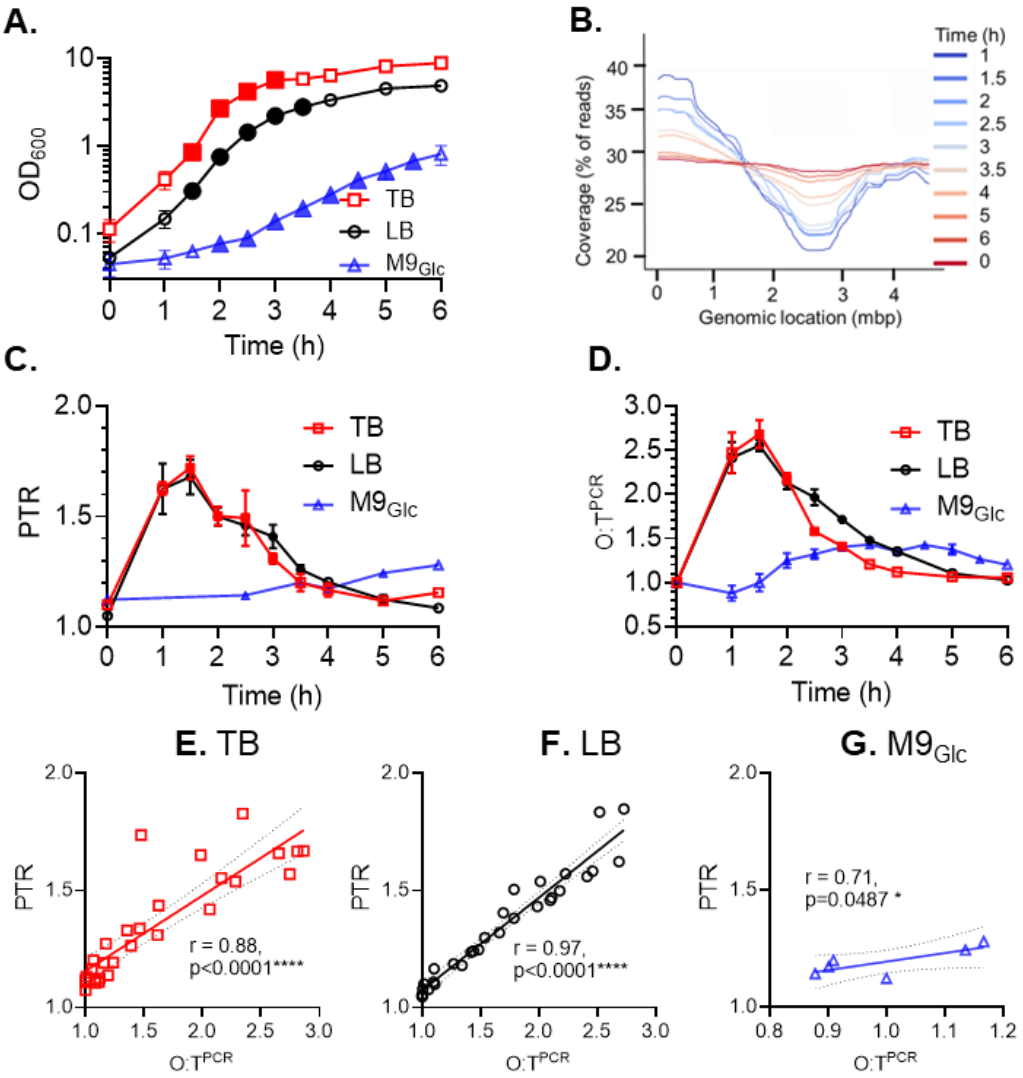

Fig. 2. Validating multiplexed quantitative PCR with whole genome sequencing as a tool for measuring origin to terminus ratios in vitro. Growth experiments of *E. coli* strain HM86 in different growth medium conditions are plotted as OD_{600} reading (A) (mean ± SD). Means and standard deviation from three independent experiments are shown for TB (red), LB (black), and $M9_{Glc}$ (blue). Three biological replicates for TB, and LB, and two biological replicates for $M9_{Glc}$. (B) illustrates the example of the sequencing coverage across the genome of HM86 grown in vitro in LB up to 6h. Genomic location of origin (*ori*) and terminus (*ter*) of replication are denoted by peak and trough respectively. PTR determined by WGS is plotted in (C) (mean ± SD). (D) plots from the $O:T^{PCR}$ values (mean ± SD). Scatterplot with linear regression for the relationship between PTR derived from WGS and *ori:ter* by qPCR method in TB (E), LB (F), and $M9_{Glc}$ (G). N= 3 replicates (TB and LB), and N=1 ($M9_{Glc}$). Pearson correlation coefficient (*r*) with *p*-values are shown in the graph. Statistical significance. **** p<.0001; *p<.05). Filled symbols in the graph A, C, and D indicates the data points with active replication included in the study for growth rate determination.

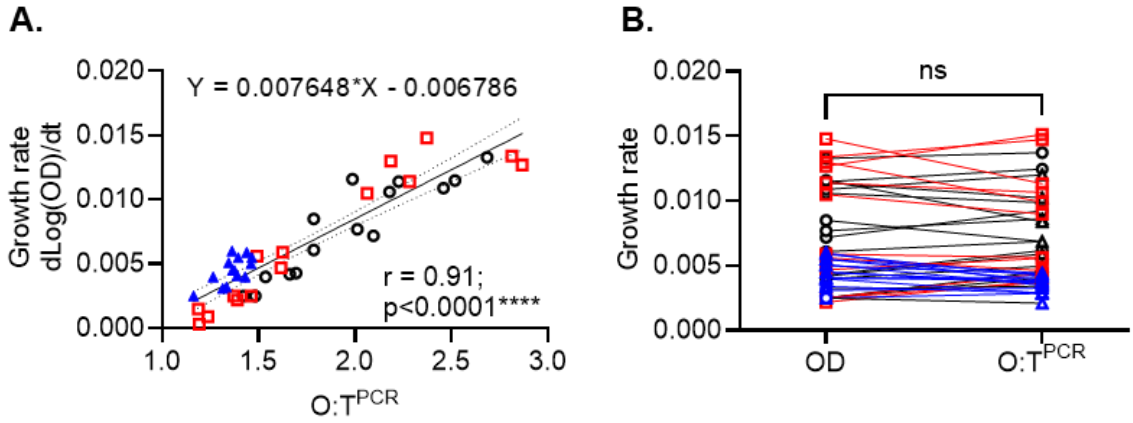

Fig. 3: Bacterial growth rate correlates with O:T^{PCR}. Graph represents the correlation between GR and *ori:ter*-values determined by qPCR method in TBLBM9$_{Glc}$ (A). TB and LB=3 biological replicates, M9$_{Glc}$= 2 biological replicates. Pearson correlation coefficient (*r*) with *p*-value is shown in the graph. Statistical significance: **** p<.0001; **p<.01). Bacterial growth rate calculated from the OD$_{600}$ reading and the qPCR$_{ori:ter}$ in TB+LB+M9$_{Glc}$ combined is plotted in Fig. B. Statistical significance was determined using the paired *t*-test, with *p*-value<0.05 considered a significant difference.

638

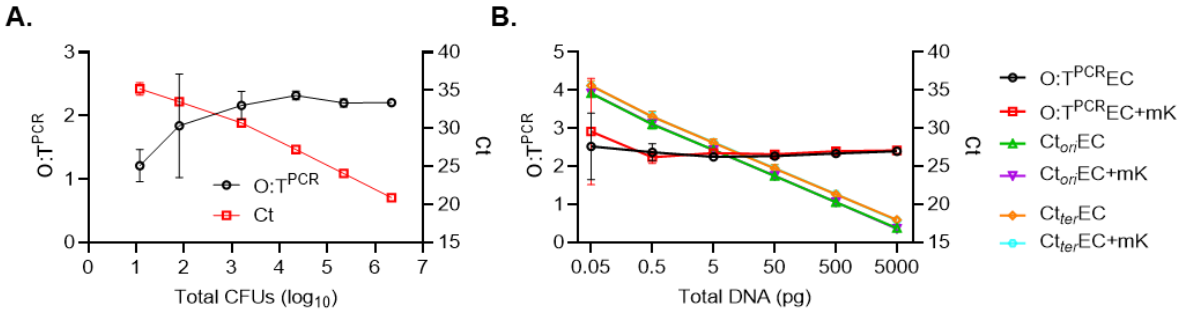

639

640 **Fig. 4: PCR assay optimization.** Standard curves (Ct vs $\log_{10}$CFU) (A), and (Ct vs total
641 DNA) (B) with their associated *ori:ter* determined by qPCR. Three replicates of the
642 bacterial culture at exponential phase of growth (time point 2 h) was used for DNA
643 extraction and determination of $O{:}T^{PCR}$ [CFU vs *ori:ter* experiment (mean ± SEM)], and
644 3 independent experiment for total DNA vs *ori:ter* (mean ± SEM). The graph depicts *E.*
645 *coli* strain HM86 *ori:ter*, Ct_{ori}, and Ct_{ter} in presence and absence of murine kidney DNA
646 (data from 3 biological replicate with 3 technical replicates) as indicated in figure
647 legends. EC (*E. coli* DNA) and mK (murine kidney DNA). DNA (data from 3 biological
648 replicates with 3 technical replicates) as indicated in figure legends. Ct (threshold cycle),
649 EC (*E. coli* DNA) and kidney (murine kidney DNA).

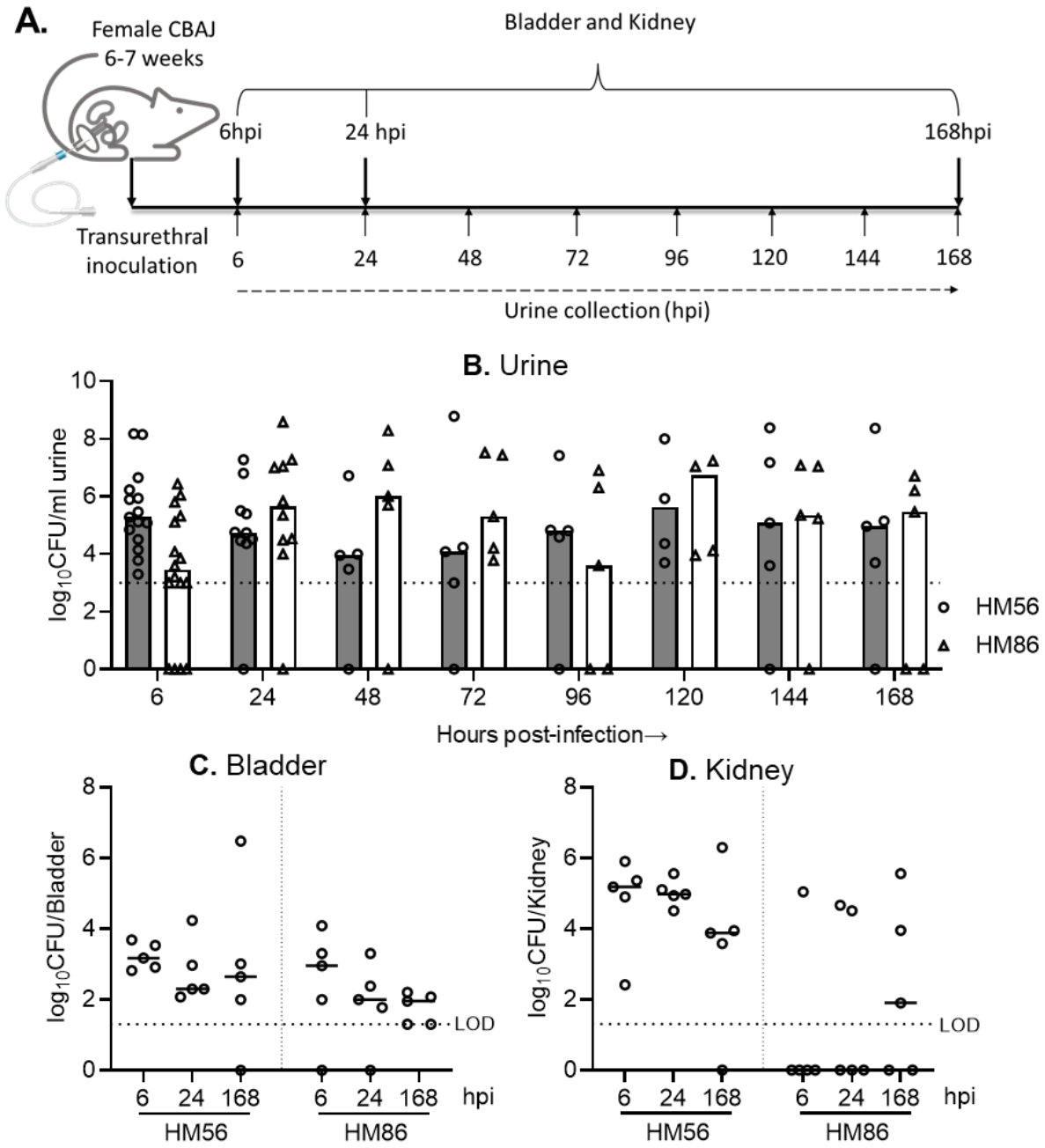

650

651 **Fig. 5: Bacterial burden in murine model of ascending UTI.** Experimental plan for
652 mouse model of ascending UTI (A)**.** CBAJ mice (n=5 per time point) were inoculated
653 with either HM56 or HM86 with ~$2*10^8$ CFU. Viable bacterial load in urine (B), bladder
654 (C) and kidneys (D) were determined by dilution plating in LB agar at specific time point
655 as mentioned in the plot. The horizontal dashed line indicates the limit of detection

656 (LOD)

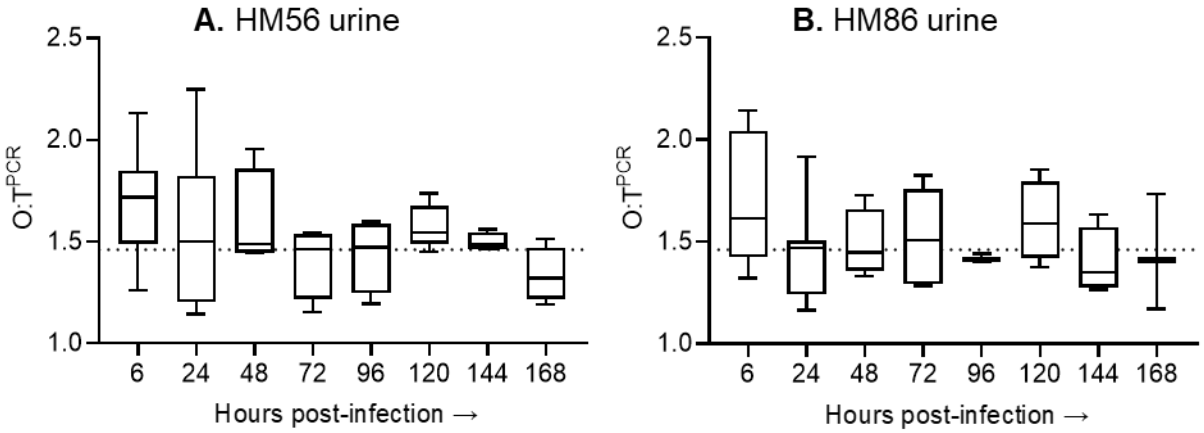

657

658 **Figure 6: O:T^{PCR} in urine samples over infection period.** Box and whiskers plots,
659 where box represents the median and interquartile ranges and whiskers represents
660 minimum and maximum values for each time during infection for HM56 (A), and HM86
661 (B). n= 5-15 mice per time point.

662

663

664

665

666

667

668

669

670

671

672

673

674

675

676

677

678 **Supplementary figures**

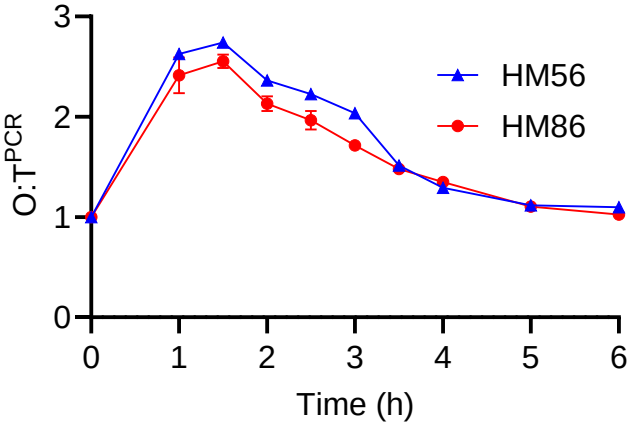

679

680 **Fig. S1. O:T^{PCR} of the UPEC strains HM86 and HM56 cultured in LB medium**. (n=3
681 for HM86, and n=1 for HM56).

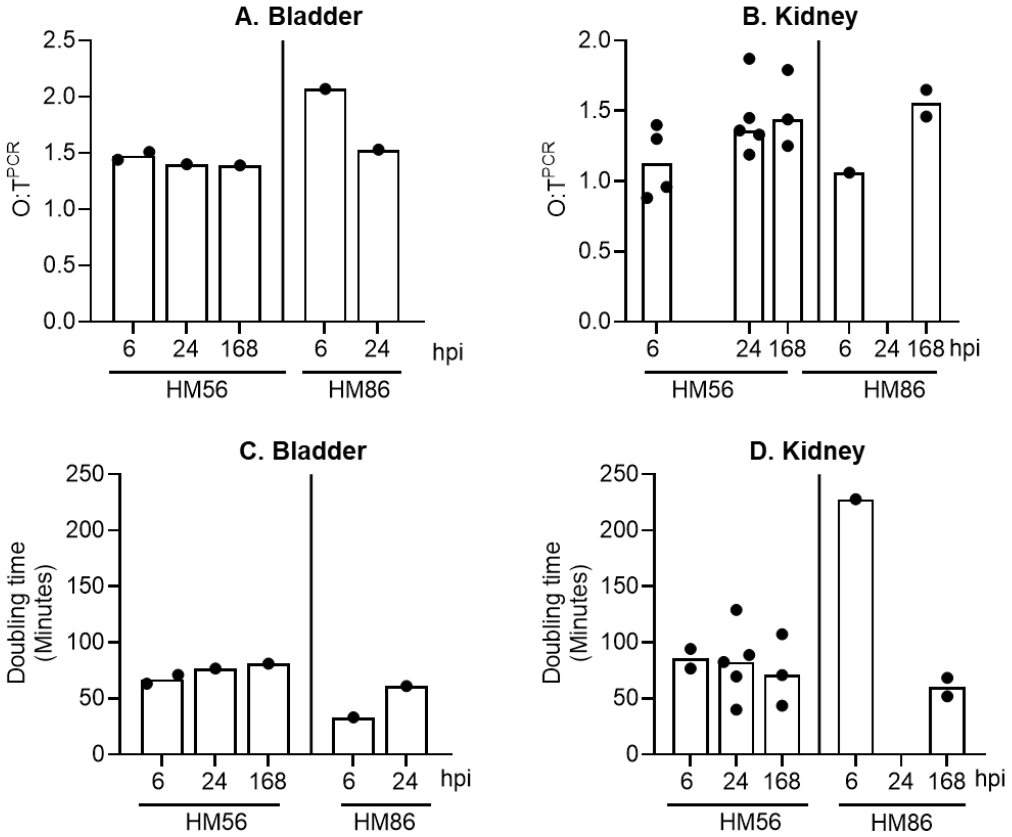

682

683 **Fig. S2. O:T^{PCR} (Bladder-A, and Kidney-B) and *E. coli* doubling time (Bladder-C,**
684 **and Kidney-D) of the mouse during experimental UTI at the time point of 6, 24,**
685 **and 168 hpi.**